Available online at www.sciencedirect.com

ScienceDirect

Geochimica et Cosmochimica Acta 165 (2015) 361–375

Geochimica et Cosmochimica Acta

www.elsevier.com/locate/gca

# Intrinsic W nucleosynthetic isotope variations in carbonaceous chondrites: Implications for W nucleosynthesis and nebular vs. parent body processing of presolar materials

Christoph Burkhardt [a,b,*], Maria Schönbächler [a]

[a] Institute of Geochemistry and Petrology, Clausiusstrasse 25, ETH Zürich, CH-8092 Zürich, Switzerland
[b] Origins Laboratory, Department of Geophysical Sciences, The University of Chicago, IL 60637, USA

Received 29 December 2014; accepted in revised form 12 June 2015; Available online 20 June 2015

**Abstract**

The progressive dissolution of the carbonaceous chondrites Orgueil (CI1), Murchison (CM2) and Allende (CV3) with acids of increasing strength reveals correlated W isotope variations ranging from 3.5 $\varepsilon^{182}$W and 6.5 $\varepsilon^{183}$W in the initial leachate (acetic acid) to −60 $\varepsilon^{182}$W and −40 $\varepsilon^{183}$W in the leachate residue. The observed variations are readily explained by variable mixing of *s*-process depleted and *s*-process enriched components. One W *s*-process carrier is SiC, however, the observed anomaly patterns and mass–balance considerations require at least on additional *s*-process carrier, possibly a silicate or sulfide. The data reveal well-defined correlations, which provide a test for *s*-process nucleosynthesis models. The correlations demonstrate that current models need to be revised and highlight the need for more precise W isotope data of SiC grains. Furthermore the correlations provide a mean to disentangle nucleosynthetic and radiogenic contributions to $^{182}$W ($\varepsilon^{182}W_{corrected} = \varepsilon^{182}W_{measured} - (1.41 \pm 0.05) \times \varepsilon^{183}W_{measured}$; $\varepsilon^{182}W_{corrected} = \varepsilon^{182}W_{measured} - (-0.12 \pm 0.06) \times \varepsilon^{184}W_{measured}$), a prerequisite for the successful application of the Hf–W chronometer to samples with nucleosynthetic anomalies.

The overall magnitude of the W isotope variations decreases in the order CI1 > CM2 > CV3. This can be interpreted as the progressive thermal destruction of an initially homogeneous mixture of presolar grains by parent-body processing. However, not only the magnitude but also the W anomaly patterns of the three chondrites are different. In particular leach step 2, that employs nitric acid, reveals a *s*-deficit signature for Murchison, but a *s*-excess for Orgueil and Allende. This could be the result of redistribution of anomalous W into a new phase by parent-body alteration, or, the fingerprint of dust processing in the solar nebula. Given that the thermal and aqueous alteration of Murchison is between the CI and CV3 chondrites, parent-body processing is probably not the sole cause for creating the different pattern. Small-scale nebular redistribution of anomalous W may have played a role as well. Similar nebular processes possibly acted differently on specific carrier phases and elements, resulting in the diverse nucleosynthetic signatures observed in planetary materials today.


## 1. INTRODUCTION

Chondritic meteorites are space sediments whose various components were produced in stellar, nebular and parent body environments (Krot et al., 2009). Isotope anomalies of nucleosynthetic origin identified for bulk rock chondrites and their components can provide key constraints on many of the involved processes and

* Corresponding author at: Institut für Planetologie, Westfälische Wilhelms-Universität Münster, Wilhelm-Klemm-Strasse 10, D-48149 Münster, Germany. Tel.: +49 251 83 33413.
*E-mail address:* burkhardt@uni-muenster.de (C. Burkhardt).

http://dx.doi.org/10.1016/j.gca.2015.06.012
0016-7037/

environments, such as stellar nucleosynthesis, physico-chemical processing and mixing of matter in the solar circumstellar disk, planetary body accretion and parent body metamorphism.

Nucleosynthetic variations in meteorites are observed on three different scales. The largest variations (isotopic deviations relative to terrestrial or average solar system composition in the % range or higher) are obtained by the direct measurements of single presolar grains isolated from the matrix of non-equilibrated chondritic meteorites (Zinner, 2014). These grains condensed around dying stars and provide a direct probe to nucleosynthetic processes occurring in their host stars and thus are invaluable samples to test and refine theoretical models of nucleosynthesis. However, these types of measurements are intricate, often associated with large uncertainties, limited to specific types of presolar grains (mainly SiC) and until now only available for certain elements (*e.g.*, Ott and Begemann, 1990; Nicolussi et al., 1997,1998; Lugaro et al., 2003; Podosek et al., 2004; Avila et al., 2012). The presence of presolar grains in chondritic meteorites provides unequivocal evidence that some primitive materials from the solar systems parental cloud survived nebular processing (Lewis et al., 1987). This implies that the solar nebula was never in complete isotopic equilibrium and thus a pure condensation origin can be excluded for most chondrite components.

Presolar grains have also been used as a proxy for parent body alteration within and between chondrite classes (*e.g.*, Huss and Lewis, 1995; Davidson et al., 2014). The findings show that the lower the amount of presolar grains within a specific chondrite of the same chondrite class, the higher is the degree of parent body alteration experienced by the meteorite. Comparison of presolar grain abundances between chondrite classes, however, is less straightforward. This is because the various presolar phases can react differently to alteration if fundamental conditions change, *e.g.*, at a given temperature SiC seems to be more stable in the reducing conditions of enstatite chondrites than in the oxidizing environment of carbonaceous chondrites (Huss and Lewis, 1995). Furthermore, as the various chondrite classes formed under different nebular (redox) conditions and vary in composition and texture, they might also sample variably processed blends of presolar materials. Therefore, the variable presolar grain abundances in the different chondrite classes might not only be due to different degrees of parent body alteration, but also indicative of varying pre-accretionary material processing in the solar nebula (Huss et al., 2003). Such processing could lead to a heterogeneous distribution of presolar materials in the solar system and might be responsible for establishing nucleosynthetic isotope variations on a planetary scale.

Planetary-scale nucleosynthetic isotope variations, that are reported for bulk chondrites and differentiated meteorites, are small (isotopic variations relative to terrestrial compositions are in the parts per $10^4$ to parts per $10^6$ range), but well resolved and established for a growing number of elements (*e.g.*, Ca, Ti, Ni, Cr, Sr, Zr, Mo, Ru, Nd, Sm) (Dauphas et al., 2002b; Andreasen and Sharma, 2007; Trinquier et al., 2007, 2009; Regelous et al., 2008; Burkhardt et al., 2011; Chen et al., 2010, 2011; Gannoun et al., 2011; Moynier et al., 2012; Akram et al., 2013, 2015). These bulk-scale anomalies are used to infer genetic relations between meteorite parent bodies and bear witness to a large-scale nebular isotopic heterogeneity that can help to better constrain material processing and mixing dynamics in the early solar system. Several models have been put forward to explain the isotopic heterogeneity among bulk meteorites. The heterogeneity could (i) reflect a primordial feature of the solar nebula inherited from a large scale heterogeneous parental molecular cloud (Clayton, 1982; Dauphas et al., 2002b), (ii) be caused by the injection of isotopically heterogeneous matter into the nebula (Lee et al., 1977), or (iii) is the result of physical and/or chemical dust processing within an initially homogeneous nebula such as *e.g.*, grain size sorting (Dauphas et al., 2010), grain type sorting (Regelous et al., 2008) or selective destruction of thermally labile presolar components in different nebular environments (Trinquier et al., 2009; Burkhardt et al., 2012a). Although the latter model is currently favored because it allows for the generation of bulk scale isotopic anomalies for some elements *and* uniform isotopic composition for others, the specific nebular processes involved are not well understood yet.

The progressive dissolution of chondritic meteorites with acids of increasing strength reveals the internal nucleosynthetic variability of chondrites. These experiments yield precise isotopic data that scale between those of single presolar grain data and those of the bulk meteorites (isotopic variations relative to terrestrial compositions are in the ‰ to parts per $10^4$ range). Currently, leachate data are available for a number of primitive chondrites (mainly carbonaceous, but also some enstatite and ordinary chondrites) and for a variety of elements including Ti, Cr, Sr, Zr, Mo, Te, Ba, Nd, Sm, W and Os (*e.g.*, Rotaru et al., 1992; Dauphas et al., 2002a; Hidaka et al., 2003; Schönbächler et al., 2003, 2005; Fehr et al., 2006; Trinquier et al., 2007, 2009; Reisberg et al., 2009; Yokoyama et al., 2010, 2011; Qin et al., 2011; Burkhardt et al., 2012a,b; Boyet and Gannoun, 2013). The leaching technique represents a quick way to establish precise nucleosynthetic isotope data for a range of elements and provide constraints on the carrier phases of the nucleosynthetic variations. The information obtained from leachates is used to test and refine nucleosynthesis models, unravel the processes that lead to the formation of bulk-scale anomalies in some elements but not in others, and address the question of nebular vs. parent body alteration. Furthermore, leachate data are needed to adequately correct nucleosynthetic anomalies in planetary materials, a prerequisite for the successful applications of some short-lived chronometers (Qin et al., 2011; Burkhardt et al., 2012b).

Previous W leachate data is limited to the carbonaceous chondrite Murchison (Burkhardt et al., 2012b). In this study, we extended this data and present W isotope data for acid leachates of the carbonaceous chondrites Orgueil (CI1), Murchison (CM2) and Allende (CV3). Aliquots from the same leach fractions were previously analyzed for Zr (Schönbächler et al., 2005) and Te (Fehr et al., 2006). The new data provide insight into nature and origin of the nucleosynthetic W isotope variations in our solar system

as well as nebular and parent body processing of presolar W materials. In addition, our results improve the precision of the leachate based correction scheme for nucleosynthetic W isotope anomalies (Burkhardt et al., 2012b) that affect the $^{182}$Hf–$^{182}$W dating system.

## 2. ANALYTICAL METHODS

### 2.1. Sample preparation and W separation

The W isotope measurements were performed on W fractions obtained from the Orgueil, Murchison and Allende leachates reported in a previous study (Schönbächler et al., 2005). The W fractions were processed through an additional clean-up chemistry here. For details on the leaching procedure and initial chemical separation see Schönbächler et al. (2005). In brief, powdered rock samples of Orgueil (1.0 g), Murchison (sample 'a'; 1.5 g) and Allende (sample 'b'; 0.825 g) were sequentially digested using the following sequence:

1: 50% HAc 1 day, 20 °C
2: 4 M $HNO_3$ 5 days, 20 °C
3: 6 M HCl 1 day, 80 °C
4: 13.5 M HF + 3 M HCl 4 days, 100 °C
5: conc. HF + $HNO_3$ 3 days, 170 °C, Teflon bomb

The leach solutions were then processed through an ion-exchange procedure developed for the chemical separation of Zr (Schönbächler et al., 2004) that also allows for the separation of W. After collection of Zr in 2 ml of 6 M HCl + 1 M HF, W was eluted from the anion columns (0.7 ml Bio-Rad AG1-X8 resin, 200–400 mesh, chloride form) with additional 3 ml of 6 M HCl + 1 M HF. The Zr cuts after the first chemistry may have contained small amounts of W (<10% of the total W). For the Orgueil and Murchison leachates this W was recovered in a Zr clean-up column, which involved the separation of Zr from Ti using $H_2SO_4$ and elution of W in 3 ml of 6 M HCl + 1 M HF (Schönbächler et al., 2004). The dried down W cuts of the leachates and the blanks obtained from the previous study were dissolved in 6 M HCl + 1 M HF and subsequently treated with $H_2O_2$–$HNO_3$ and aqua regia to destroy organic compounds eluted from the resin. The W cuts from the first and second Zr ion exchange column were combined and blanks were spiked with a $^{183}$W tracer. Following previously established techniques (Kleine et al., 2004), the W cuts were then purified by anion-exchange chromatography (1 ml Bio-Rad AG1-X8, 200–400 mesh) in a HCl-HF media. After cleaning and conditioning of the columns the samples were loaded in 4 ml 0.5 M HCl + 0.5 M HF. The matrix was rinsed with 5 ml 0.5 M HCl + 0.5 M HF, 4.5 ml 8 M HCl + 0.01 M HF and 0.5 ml 6 M HCl + 1 M HF before W was collected in 4.5 ml 6 M HCl + 1 M HF. Finally, the samples were dried down, taken up in 0.5 M $HNO_3$ + 0.05 M HF and were ready for analysis. Total procedural blanks were 0.70, 0.27, 0.24, 0.19 and 0.47 ng for the leach steps 1–5, resulting in significant blank corrections for leach step 1 and 5 for all meteorites (around 10%, except for Orgueil leachate 1, Murchison leachate 1 and Allende leachate 5 with 180%, 27% and 70% blank correction, respectively). A terrestrial W isotope composition and an uncertainty of 50% were assumed for the blank correction (Table 1).

### 2.2. Mass spectrometry

Tungsten isotope measurements of the leachates were performed using the Thermo *NeptunePlus* MC-ICPMS (multiple collector inductively coupled plasma mass spectrometer) at the Institut für Planetologie, University of Münster, Germany. Samples were introduced via a Cetac Aridus II desolvating unit equipped with a self-aspirating PFA-nebulizer. A standard (H) cone setup and a nebulizer uptake rate of ~100 µl/min resulted in ion beam intensities of $1 \times 10^{-11}$ A on $^{183}$W for a 30 ppb W solution. Tungsten isotope compositions of the leachate samples were typically measured at ion beam intensities between $2 \times 10^{-12}$ and $1 \times 10^{-11}$ A on $^{183}$W. Due to their low W content, Orgueil leachate 1 and Allende leachate 5 were measured with signal sizes of $1 \times 10^{-12}$ and $8 \times 10^{-13}$ A on $^{183}$W, respectively. Each measurement consisted of 60 s baseline integrations (deflected beam) followed by 40 isotope ratio measurements using 4.2 s each. Isobaric Os interferences on $^{184}$W and $^{186}$W were corrected by monitoring interference-free $^{188}$Os. Interference corrections were generally <10 ppm and always <70 ppm (Orgueil leachate 5). Instrumental and natural mass bias was corrected by internal normalization to $^{186}W/^{184}W = 0.92767$ or $^{186}W/^{183}W = 1.98594$ (Völkening et al., 1991) using the exponential law. The W isotope analyses of the samples were bracketed by measurements of a terrestrial W standard solution (Alfa Aesar, 20 or 30 ppb) and are reported as $\varepsilon^i$W, which is the part per $10^4$ deviation of the $^iW/^{18j}W$ isotope ratio ($i = 182; 183; 184$ and $j = 3; 4$) from the mean of the bracketing standard runs. The external reproducibility (2 s.d.) of the 30 ppb standard solution was estimated from 10 consecutive standard runs measured before the sample-standard bracketing sequence to ±0.2 $\varepsilon^{182}$W and ±0.3 $\varepsilon^{183}$W for normalization relative to $^{186}W/^{184}W$ and ±0.4 $\varepsilon^{182}$W and ±0.3 $\varepsilon^{184}$W for normalization relative to the $^{186}W/^{183}W$ ratio. Reported uncertainties for samples measured once are 2 s.e. internal error or the external reproducibility (2 s.d.) of the standard measured the same day, whichever is larger. For samples measured twice, the $2\sigma$ weighted average or the external reproducibility (2 s.d.) of the standard are reported, whichever is larger, and for samples measured three or more times the 95% Student-$t$ confidence intervals ($\sigma t_{0.95,n-1}/\sqrt{n}$).

Aliquots from the initial leachate solutions were not available for this study and therefore no precise initial W (and Hf) concentrations of the unprocessed leachate solutions could be determined. Nevertheless, W concentrations of the leachate samples were obtained by comparing the sample signal intensities with those of a W standard solution with known concentration by MC-ICPMS after ion-exchange chemistry. The uncertainty of this method is estimated to be ~20%. The absolute concentrations obtained this way bear little significance because the yield of the column chemistry was significantly lower than

Table 1
W concentrations and isotopic compositions for acid leachates of Orgueil, Murchison and Allende.

| Sample | Step | $f$W[a] | W[b] [ng/g] | $N$[c] | $\varepsilon^{182}$W[d] $\pm 2\sigma$ | $\varepsilon^{183}$W $\pm 2\sigma$ | $\varepsilon^{184}$W | $\varepsilon^{186}$W | $\varepsilon^{182}W_{corrected}$[e] $\pm 2\sigma$ | $\varepsilon^{182}$W $\pm 2\sigma$ | $\varepsilon^{183}$W | $\varepsilon^{184}$W $\pm 2\sigma$ | $\varepsilon^{186}$W | $\varepsilon^{182}W_{corrected}$[e] $\pm 2\sigma$ |
|---|---|---|---|---|---|---|---|---|---|---|---|---|---|---|
| *Orgueil (CI1)* | | | | | Normalized to $^{186}W/^{183}W = 0.92767$ | | | | | Normalized to $^{186}W/^{183}W = 1.98594$ | | | | |
| 50% HAc | 1 | 0.01 | 0.4 | 1 | 3.53 ± 2.08 | 6.42 ± 2.77 | 0 | 0 | −5.53 ± 4.44 | −4.40 ± 2.39 | 0 | −4.27 ± 1.84 | 0 | −4.91 ± 2.41 |
| 4M HNO3 | 2 | 0.11 | 6.5 | 1 | −10.38 ± 0.64 | −6.88 ± 0.59 | 0 | 0 | −0.68 ± 1.10 | −1.29 ± 0.57 | 0 | 4.58 ± 0.39 | 0 | −0.74 ± 0.62 |
| 6M HCl | 3 | 0.21 | 13.0 | 2 | −1.95 ± 0.50 | 0.19 ± 1.10 | 0 | 0 | −2.22 ± 1.64 | −2.26 ± 1.11 | 0 | −0.13 ± 0.73 | 0 | −2.27 ± 1.12 |
| 3M HCl + 13.5M HF | 4 | 0.59 | 36.5 | 4 | 6.91 ± 0.44 | 6.49 ± 0.63 | 0 | 0 | −2.24 ± 1.04 | −1.91 ± 0.86 | 0 | −4.31 ± 0.42 | 0 | −2.43 ± 0.89 |
| Teflon bomb | 5 | 0.08 | 5.2 | 1 | −59.60 ± 2.58 | −40.52 ± 1.79 | 0 | 0 | −2.47 ± 4.14 | −5.41 ± 0.99 | 0 | 27.04 ± 1.19 | 0 | −2.17 ± 1.68 |
| Total or wt. av. | | | 61.7 | | −2.44 ± 0.57 | −0.23 ± 0.84 | 0 | 0 | −2.11 ± 1.31 | −2.23 ± 0.90 | 0 | 0.16 ± 0.56 | 0 | −2.21 ± 0.91 |
| *Murchison-a (CM2)* | | | | | | | | | | | | | | |
| 50% HAc | 1 | 0.03 | 1.7 | 1 | 1.17 ± 1.08 | 3.05 ± 1.13 | 0 | 0 | −3.14 ± 1.93 | −2.78 ± 1.27 | 0 | −2.03 ± 0.75 | 0 | −3.02 ± 1.28 |
| 4M HNO3 | 2 | 0.24 | 15.7 | 3 | −0.93 ± 0.49 | 1.71 ± 0.41 | 0 | 0 | −3.33 ± 0.77 | −3.04 ± 1.20 | 0 | −1.14 ± 0.28 | 0 | −3.18 ± 1.20 |
| 6M HCl | 3 | 0.21 | 13.9 | 3 | −0.44 ± 0.93 | 1.30 ± 0.73 | 0 | 0 | −2.28 ± 1.39 | −2.21 ± 0.53 | 0 | −0.87 ± 0.49 | 0 | −2.32 ± 0.54 |
| 3M HCl + 13.5M HF | 4 | 0.46 | 29.6 | 3 | −0.65 ± 0.59 | 0.31 ± 0.57 | 0 | 0 | −1.08 ± 0.99 | −1.09 ± 0.68 | 0 | −0.20 ± 0.38 | 0 | −1.11 ± 0.69 |
| Teflon bomb | 5 | 0.06 | 4.1 | 1 | −29.35 ± 1.25 | −19.17 ± 0.86 | 0 | 0 | −2.32 ± 1.99 | −3.58 ± 0.65 | 0 | 12.77 ± 0.57 | 0 | −2.05 ± 0.91 |
| Total or wt. av. | | | 65.0 | | −2.43 ± 0.69 | −0.30 ± 0.60 | 0 | 0 | −2.01 ± 1.09 | −2.00 ± 0.79 | 0 | 0.20 ± 0.40 | 0 | −1.98 ± 0.79 |
| *Allende-b (CV3)* | | | | | | | | | | | | | | |
| 50% HAc | 1 | 0.10 | 7.1 | 1 | −2.50 ± 0.50 | 0.31 ± 0.35 | 0 | 0 | −2.94 ± 0.70 | −2.74 ± 0.60 | 0 | −0.21 ± 0.24 | 0 | −2.77 ± 0.60 |
| 4M HNO3 | 2 | 0.18 | 13.1 | 3 | −3.78 ± 0.87 | −1.09 ± 0.77 | 0 | 0 | −2.24 ± 1.39 | −2.20 ± 0.29 | 0 | 0.73 ± 0.51 | 0 | −2.11 ± 0.30 |
| 6M HCl | 3 | 0.22 | 16.6 | 3 | −1.49 ± 0.66 | 0.07 ± 1.05 | 0 | 0 | −1.58 ± 1.62 | −1.57 ± 1.05 | 0 | −0.05 ± 0.70 | 0 | −1.58 ± 1.05 |
| 3M HCl + 13.5M HF | 4 | 0.49 | 36.4 | 3 | −1.21 ± 0.78 | 0.10 ± 0.27 | 0 | 0 | −1.36 ± 0.86 | −1.52 ± 0.87 | 0 | −0.07 ± 0.18 | 0 | −1.52 ± 0.87 |
| Teflon bomb | 5 | 0.01 | 0.8 | 1 | −5.88 ± 2.14 | −1.77 ± 2.00 | 0 | 0 | −3.38 ± 3.55 | −2.92 ± 2.58 | 0 | 1.18 ± 1.33 | 0 | −2.78 ± 2.58 |
| Total or wt. av. | | | 74.0 | | −1.90 ± 0.75 | −0.12 ± 0.56 | 0 | 0 | −1.74 ± 1.09 | −1.78 ± 0.80 | 0 | 0.08 ± 0.37 | 0 | −1.77 ± 0.80 |

[a] Fraction of total released W.

[b] W concentrations determined after ion-exchange chemistry by MC-ICPMS. Relative uncertainty of this method is estimated to be ~20%.

[c] Number of isotopic analyses of a sample.

[d] W isotope ratios are reported as deviations from the terrestrial standard: $\varepsilon^{i}W = [(^{i}W/^{18x}W)_{sample}/(^{i}W/^{18x}W)_{standard} - 1] \times 10^{4}$, with $x = 3;4$ for internal normalization to $^{186}W/^{183}W = 1.98594$ or $^{186}W/^{184}W = 0.92767$, respectively. Uncertainties represent internal error (2 se) for $N = 1$, weighted average (2 se) for $N = 2$ and two-sided 95% Student-$t$ distributions ($t_{0.95,n-1}\sigma/\sqrt{n}$) for $N > 2$ and include a propagated 50% uncertainty for the blank correction (where significant). The blank correction assumes a terrestrial composition of the blank and is given by $\varepsilon^{18x}W_{blank\ corr} = \varepsilon^{18x}W_{measured}\ (1 + {}^{blank}/_{sample})$, where ${}^{blank}/_{sample}$ is the ratio of the W amounts in the blank and the sample. The uncertainty on the blank corrected values is given by $2\sigma^2_{blank\ corr} = 2\sigma^2_{measured} + ((\varepsilon^{18x}W_{blank\ corr} - \varepsilon^{18x}W_{measured}) \times 0.5)^2$.

[e] $\varepsilon^{182}$W corrected for nucleosynthetic effect using $\varepsilon^{182}W_{corrected} = \varepsilon^{182}W_{measured} - (1.41 \pm 0.05) \times \varepsilon^{183}W_{measured}$; $\varepsilon^{182}W_{corrected} = \varepsilon^{182}W_{measured} - (-0.12 \pm 0.06) \times \varepsilon^{184}W_{measured}$.

100%. However, assuming that the relative W loss through ion-exchange chemistry was about constant for all samples, the obtained relative W abundances can still be used to constrain the W release patterns and to calculate weighted average W isotopic compositions of the bulk chondrites (see below).

## 3. RESULTS

The W concentrations and isotope data of the investigated carbonaceous chondrite leachates are presented in Table 1 and Figs. 1–3. The measured W concentrations of the leachates after ion-exchange chemistry sum up to 61.7 ng/g for Orgueil, 65.0 ng/g for Murchison and 74.0 ng/g for Allende (Table 1), which is about half of the actual W concentration of these samples (116.8, 133.6 and 167.8 ng/g; Kleine et al., 2004). This indicates a W yield of ~50% for the ion-exchange procedures, somewhat lower than what is obtained in other W studies, but acceptable when considering that the samples were processed through an initial chemistry optimized for Zr. The fractional W release patterns obtained from the concentration data are broadly similar for all investigated meteorites (Fig. 1). Less than 10% of the total W content is released in leach step 1 and 5, around 20% in step 2 and 3 and the major W fraction is collected in step 4. Although the uncertainties on the W release patterns are high, there appears to be a systematic trend for step 1 and 5, when the different chondrite groups are compared. For leach step 1, the amount of W released increases in the order CI1 < CM2 < CV3, while step 5 shows a decrease in the same order (CI1 > CM2 > CV3).

The $\varepsilon^{i}$W values are shown for internal normalization relative to $^{186}W/^{184}W$ and $^{186}W/^{183}W$ (Table 1, Fig. 2). Any $\varepsilon^{i}$W variations represent the net effect of all W isotopes involved in that particular normalization scheme and this explains the different anomaly patterns observed for the two normalization schemes. Most leachates exhibit anomalous W isotope compositions. The largest anomalies in each meteorite are observed for step 5, while the size of the anomalies revealed by step 5 decrease in the order CI1 > CM2 > CV3. The weighted averages of the W isotope compositions of the different leach steps are isotopically normal for all samples (*i.e.*, chondritic −2 $\varepsilon^{182}$W and ~0 for all non-radiogenic W isotopes), consistent with bulk rock measurements (Kleine et al., 2004). This indicates that all important nucleosynthetic W carriers were sampled by the leach experiment (Fig. 2). Not only the magnitude of the isotope anomalies varies between the different chondrite groups, but also the overall anomaly release pattern along the leachate sequence. While a continuous decrease from positive $\varepsilon^{183}$W for leach step 1 to negative $\varepsilon^{183}$W for step 5 is observed for Murchison, neither Orgueil nor Allende show this pattern (Figs. 2 and 6). This is unlikely the result of an analytical artifact, because $\varepsilon^{183}$W and $\varepsilon^{182}$W values of the different leachates are well correlated ($R^2 = 0.99$) (Fig. 3).

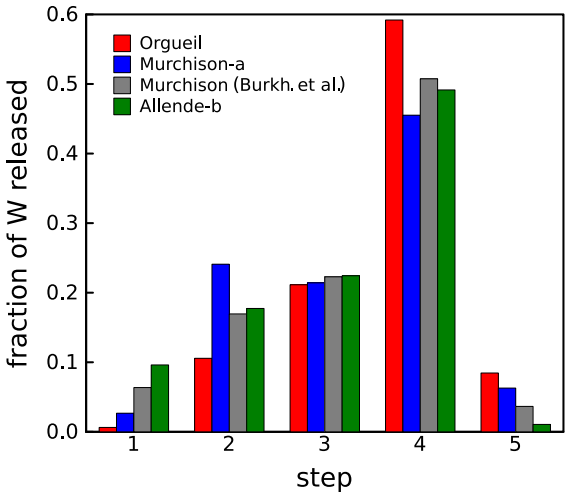


Fig. 1. Fraction of W released in the different leach steps. Overall the release patterns are broadly similar for all chondrites examined. Also shown are the Murchison leachate data from Burkhardt et al. (2012b).

## 4. DISCUSSION

### 4.1. Comparison to previous W leachate data

The W isotope variations reveal the presence of isotopically diverse components in all of the investigated carbonaceous chondrites. The elemental release pattern as well as the isotope data obtained here for the Murchison leachates (Figs. 1 and 3) are in very good agreement with a previous W leach experiment on this meteorite (Burkhardt et al., 2012b). This highlights the robustness of the data and the absence of analytical artefacts in our measurements, because the two studies used different samples of Murchison, which were digested following slightly different protocols. Moreover, W was separated using distinct ion-exchange procedures, and the measurements were performed on different MC-ICPMS instruments (Nu *Plasma* and Thermo *NeptunePlus*). The good agreement of the studies indicates that digestion of the leachate residue in Parr bombs (leach step 5) is sufficient to release all anomalous W from highly refractory phases. Therefore, fusion of the residue by laser (*cf.*, Burkhardt et al., 2012b) is not required for this element. Furthermore, the common elemental release pattern (Fig. 1) and the identical weighted average isotopic compositions (*i.e.*, chondritic $\varepsilon^{182}W \sim -2$ and $\varepsilon^{183}W$, $\varepsilon^{184}W$ ~0) of both studies imply that although the W concentrations were not measured before ion exchange chemistry in the current study and yields were only ~50%, the obtained relative W abundances are sufficiently accurate such that they can be used to constrain the W release patterns and calculate weighted averages of isotopic compositions.

### 4.2. Origin of W isotope variations and implications for nucleosynthesis models

The upper panel of Fig. 4 is showing the *s*- and *r*-process pathways in the W mass region. While $^{180}W$ is mainly produced by the *p*-process, the other W isotopes are

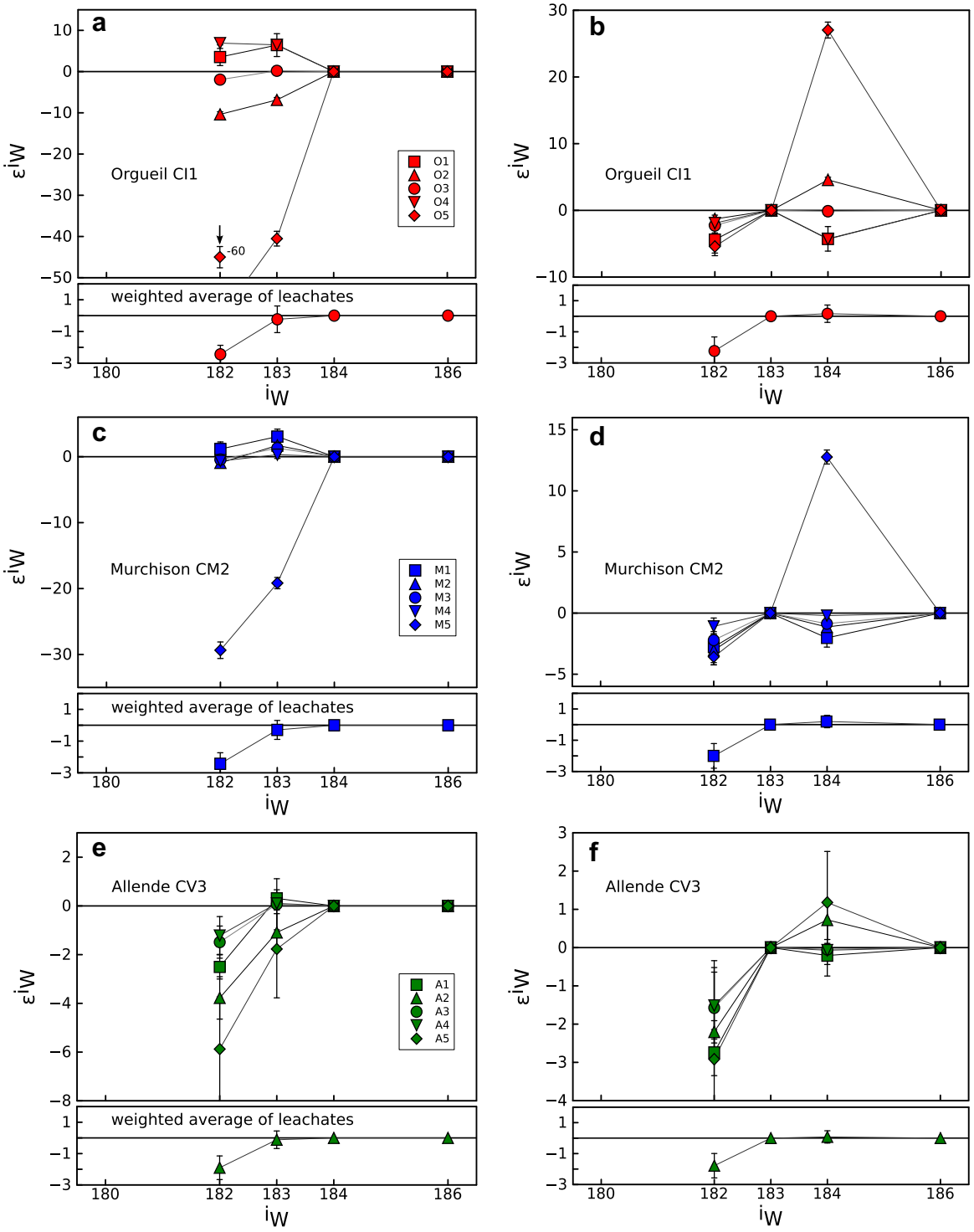


Fig. 2. W isotope data for leachates from Orgueil (a, b), Murchison (c, d) and Allende (e, f) for internal normalization to $^{186}W/^{184}W$ (a, c, e) and $^{186}W/^{183}W$ (b, d, f). Most leachates exhibit anomalous W isotope compositions consistent with variable excesses and deficits in *s*-process W. For a given meteorite the largest anomalies are observed for step 5, while between the different meteorites the size of the anomalies decrease in the order CI > CM > CV (note different scales). The weighted average of the W isotope compositions of the different leach steps is isotopically normal for all samples (*i.e.*, $\sim -2$ for $\varepsilon^{182}W$ and $\sim 0$ for all non-radiogenic W isotopes).

synthesised by both, the *s*- and the *r*-processes. In principle, the *s*- and *r*-process contributions to the solar W isotope abundances can be quantified through *s*-process model calculations. However, the various *s*-process branching points ($^{181}Hf$, $^{182}Hf$, $^{182}Ta$, $^{183}Ta$, $^{185}W$), whose stellar decay rates and activation dependency on stellar mass

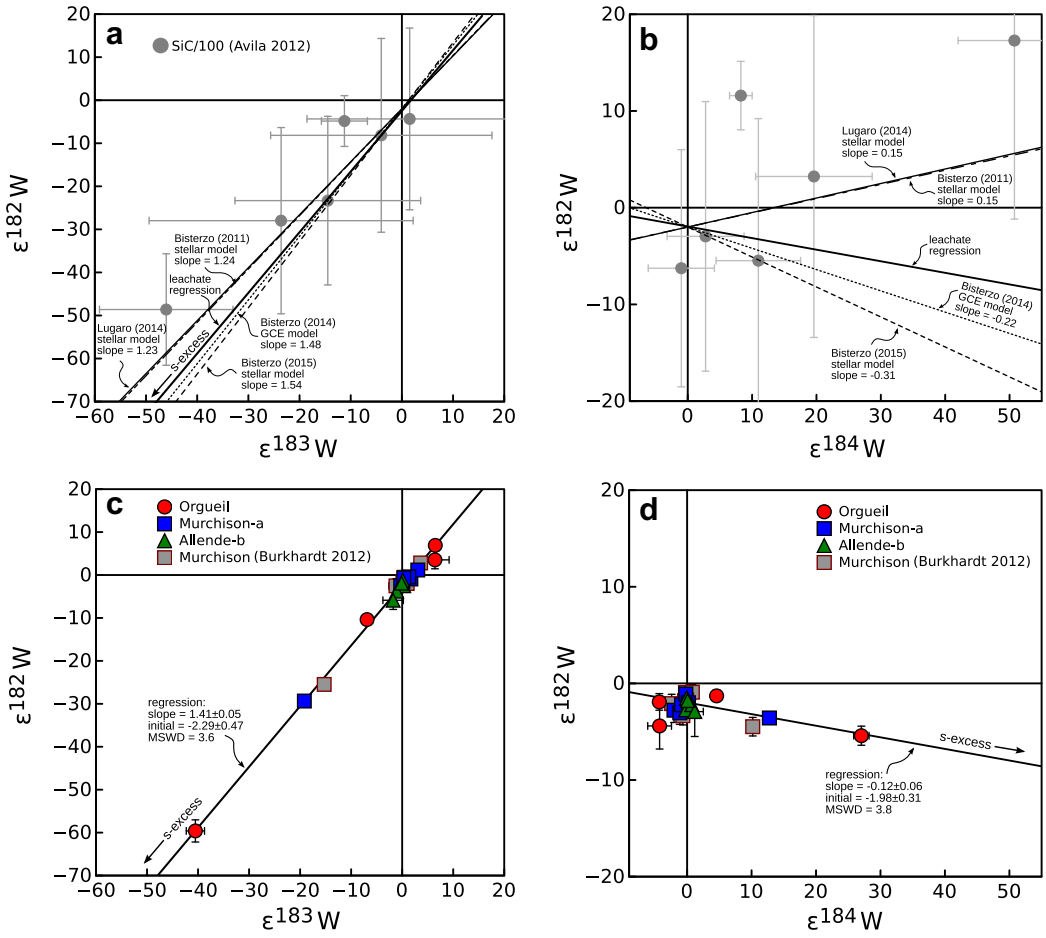


Fig. 3. $\varepsilon^{182}W$ vs. $\varepsilon^{183}W$ and $\varepsilon^{182}W$ vs. $\varepsilon^{184}W$ diagrams. (a, b) SiC data (divided by 100; with $2\sigma$ uncertainties; Avila et al., 2012) and various mixing lines between average solar system W and *s*-process W as obtained from recent *s*-process model calculations (Bisterzo et al., 2011, 2014, 2015; Lugaro et al., 2014) show some variation around the precise regressions defined by leachate data of Orgueil, Murchison and Allende (c, d). The regressions are interpreted to define mixing lines between average solar system and solar *s*-process W.

and metallicity are not well known, render *s*-process nucleosynthesis calculations in the W mass region challenging and model dependent. Furthermore, since the composition of the solar system is the result of various generations of AGB stars with variable sizes, an integrated approach must be considered to model the cosmic solar *s*-process component. Nevertheless, the W *s*-process yields for different recent stellar (Bisterzo et al., 2011, 2015; Lugaro et al., 2014) and galactic chemical evolution models (Bisterzo et al., 2014) are broadly consistent (Fig. 4, lower panel) and thus should represent a good first approximation of the average solar system W *s*-process composition. Most variations among the models are in the $^{182}W$ and $^{186}W$ yields. This is due to uncertainties in the branching factors of $^{181}Hf$ and $^{185}W$. Note that the $^{182}W$ *s*-yields of the models discussed here include $^{182}Hf$ that was produced in the *s*-process. Using the modeled W *s*-process production ratios, an excess in *s*-process W relative to the terrestrial isotope composition results in negative $\varepsilon^{182}W$ and $\varepsilon^{183}W$ values for internal normalization relative to $^{186}W/^{184}W$, with $\varepsilon^{182}W/\varepsilon^{183}W$ ratios ranging from 1.23 for the model of Lugaro et al. (2014) to 1.54 for the model of Bisterzo et al. (2015) (Fig. 3a). Likewise, internal normalization relative to $^{186}W/^{183}W$ results in slopes ranging from +0.15 to −0.31 in the $\varepsilon^{182}W$–$\varepsilon^{184}W$ diagram (Fig. 3b) for the model of Lugaro et al. (2014) and Bisterzo et al. (2015), respectively. Tungsten isotope data from single SiC grains (Avila et al., 2012) also fall on or close to these correlations, adding further evidence that the model calculations are a good first approximation of the solar *s*-process W. A direct comparison of the SiC data with the modeled slopes might be misleading, however, because the initial amount of $^{182}Hf$ in SiC grains is not known. Measured ratios indicate a subchondritic Hf/W ratios for these grains (Avila et al., 2012), and thus only little *s*-process $^{182}W$ from the $^{182}Hf$ decay. However, caution should be used when interpreting the W data from SiC grains because their separation was performed using polytungstate liquids (Amari et al., 1994) and W contamination cannot be excluded. In any case, the large uncertainties of the SiC grain data prevent drawing strong conclusions on the W *s*-process.

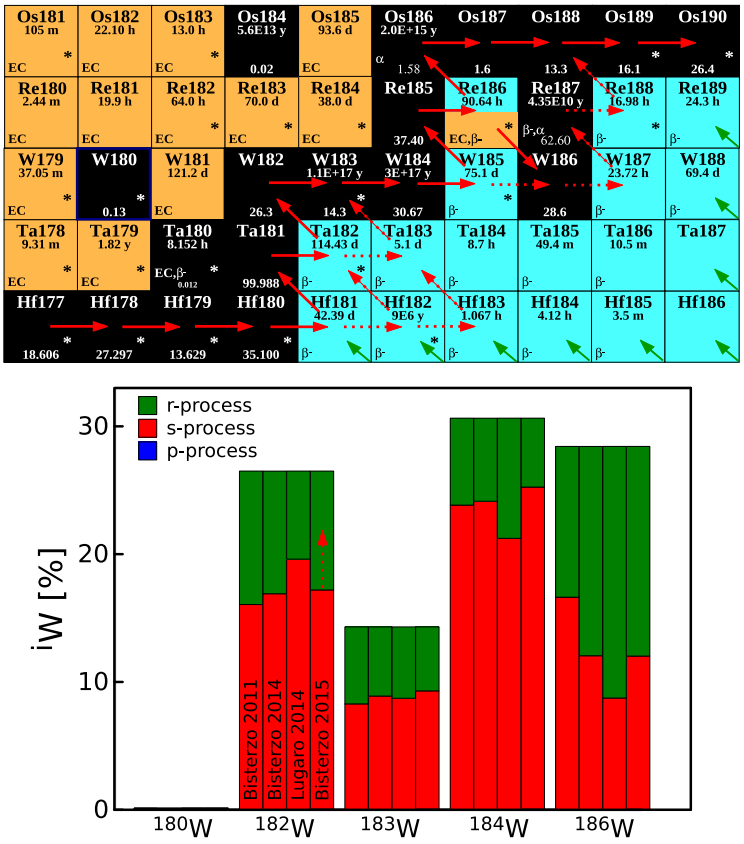


Fig. 4. The W region of the chart of the nuclides (upper panel) and estimates of the nucleosynthetic contributions to the W isotope abundances (lower panel). Stable isotopes and their solar abundances are in black boxes, short-lived isotopes and their half-lives are in blue ($\beta^-$unstable) and orange (electron capture). The red arrows indicate the main path of *s*-process nucleosynthesis, dashed arrows minor branches. Green arrows mark the decay path of nuclides produced in the *r*-process. The isotope $^{180}$W is produced by the *p*-process, $^{182}$W, $^{183}$W, $^{184}$W and $^{186}$W are produced by the *s*- and the *r*-processes. Nucleosynthetic contributions to the different W isotopes are given for four recent *s*-process calculations: Bisterzo et al. (2011, 2014, 2015) and Lugaro et al. (2014). (For interpretation of the references to color in this figure legend, the reader is referred to the web version of this article.)

Compared to the SiC data, the anomalies of the leachates are about a 100 times smaller, but a factor ~1000 more precise (Fig. 3). The leachate data fall within the range defined by the *s*-process model predictions and exhibit a well-defined positive correlation with a slope of $1.41 \pm 0.05$ and a *y*-intercept of $-2.29 \pm 0.47$ in a $\varepsilon^{182}$W vs. $\varepsilon^{183}$W diagram (Fig. 3c), and a negative slope of $-0.12 \pm 0.06$ and an intercept of $-1.98 \pm 0.31$ in the $\varepsilon^{182}$W vs. $\varepsilon^{184}$W diagram, respectively (Fig. 3d). The leachate W isotope variations are therefore best explained by the presence of one or more carriers of *s*-process W that were admixed with *s*-process depleted/*r*-process enriched components (distinction between *s*-deficit and *r*-excess would require precise $\varepsilon^{180}$W data, which could not be obtained in this study due to the low abundance of this isotope). Provided that the leachates are characterized by roughly chondritic Hf/W ratios, and thus $^{182}$Hf decay is not significantly affecting the slopes (see detailed discussion of this issue in Section 4.3), the deviations of the best fit lines for the leachates from the model predictions suggest that the modeled W *s*-process yields are imperfect descriptions of the solar cosmic W *s*-process abundances. Assuming that the deviations are either in $^{182}$W or $^{186}$W (the isotopes for which the *s*-process model results vary most significantly), the slopes of the model prediction become identical to those defined by the leachates, when the $^{182}$W or $^{186}$W *s*-process yields are adjusted from 60.6% and 58.5% to 55.5% and 41.5% for Bisterzo et al. (2011), from 64.9% and 42.3% to 70% and 58.8% for Bisterzo et al. (2015), from 74% and 30.8% to 69% and 14% for Lugaro et al. (2014) and from 63.8% and 42.4% to 66.2% and 50.6% for Bisterzo et al. (2014), respectively. Which of the isotopes (or combination of isotopes) is eventually responsible for the mismatch of the model predictions and the leachate data is difficult to assess because the evolutionary *s*-process calculations are affected by many uncertainties such as *e.g.*, the formation and size of the $^{13}$C pocket, the efficiency of the $^{22}$Ne neutron source and the accuracy of stellar half-lives and neutron capture cross-sections. Comparing the W yields of Bisterzo et al. (2011) and Bisterzo et al. (2015) shows that even within essentially the same stellar model the uncertainties are significant. Currently, the GCE model of Bisterzo et al. (2014) shows the best agreement with the leachate data.

In summary, the above observations highlight that solar W *s*-process model predictions require further improvement. Although a direct and unique inversion of the leachate data to obtain true cosmic *s*-process yields is not possible due to the internal normalization scheme required for instrumental mass-bias correction, the leachate data provide precise information for testing and refining of future *s*-process model calculations in the Hf–Ta–W–Os mass region. Hence, the *s*-process yields obtained in future model calculations, that aim to match the solar abundance pattern can only be accurate if they fit the leachate data.

### 4.3. Implications for the $^{182}$Hf–$^{182}$W dating system

Considerable interest in studying W isotopes is related to the short-lived $^{182}$Hf–$^{182}$W decay system ($t_{1/2} = 8.9$ Ma, Vockenhuber et al., 2004), which has proven to be a versatile chronometer of early solar system processes (*e.g.*, Kleine et al., 2009). The application of the Hf–W system to establish the relative timing of events in the early solar system thus requires a rigorous assessment of any nucleosynthetic W isotope variability in early solar system materials. It is evident that any differences in parent or daughter isotope ratios that are not the result of radioactive decay but are of nucleosynthetic origin will lead to incorrect ages. Thus far, however, besides a small *s*-deficit in IVB iron meteorites ($\varepsilon^{184}W = -0.08$; Qin et al., 2008) no nucleosynthetic W isotope anomalies have been observed at the bulk meteorite scale. This implies that the distinct presolar W carriers were well homogenized in the nebula at the time the meteorite parent bodies formed. The use of the Hf–W chronometer to date events on a bulk meteorite and planetary scale is therefore not significantly compromised by nucleosynthetic W isotope anomalies. However, accurate and precise Hf–W dating requires knowledge of the solar system initial $^{182}$Hf/$^{180}$Hf and $\varepsilon^{182}$W values, which are most readily determined through the investigation of Ca–Al-rich inclusions (CAI) (Burkhardt et al., 2008). These refractory element-rich inclusions contained in chondritic meteorites are generally used to define the start of solar system and form an important time anchor for short- and long-lived chronometers (*e.g.*, Nyquist et al., 2009; Amelin et al., 2010). However, they also exhibit nucleosynthetic anomalies for a variety of elements, including W (Burkhardt et al., 2008, 2012b; Kruijer et al., 2014). Therefore, these samples need to be corrected for nucleosynthetic W isotope variations before precise and accurate initial $^{182}$Hf/$^{180}$Hf and $\varepsilon^{182}$W values for our solar system can be constrained.

Several methods can be used to quantify the effects of nucleosynthetic anomalies on $\varepsilon^{182}$W. They all employ the anomalies measured in non-radiogenic W isotopes (*i.e.*, $\varepsilon^{183}$W; $\varepsilon^{184}$W) and an estimate of their nucleosynthetic relationship with $\varepsilon^{182}$W to obtain anomaly corrected $\varepsilon^{182}$W values. Theoretical models of *s*-process nucleosynthesis or SiC data can provide such estimates (*cf.*, Section 4.2). However, as the *s*-process path in the W mass range is not well understood and SiC data are not very precise, these estimates are associated with large uncertainties. An improved way to correct nucleosynthetic anomalies on $\varepsilon^{182}$W was put forward by Burkhardt et al. (2012b). These authors used leachate data as well as decay-corrected CAI data to obtain the correction equations of $\varepsilon^{182}W_{corr} = \varepsilon^{182}W_{measured} - 1.53 \pm 0.13 \times \varepsilon^{183}W$ (from the leachate regression) and $\varepsilon^{182}W_{corr} = \varepsilon^{182}W_{measured} - 1.48 \pm 0.24 \times \varepsilon^{183}W$ (from the CAI regression), which led to a significant downward revision of the solar system initial $\varepsilon^{182}$W from $-3.28 \pm 0.12$ to $-3.51 \pm 0.10$. The leachate data presented here span over an about twice as large anomaly range and therefore allow for even tighter constraints for the correction scheme. Regressions of all leachate data in $\varepsilon^{182}$W vs. $\varepsilon^{183}$W and $\varepsilon^{182}$W vs. $\varepsilon^{184}$W space yield relations of

$$\varepsilon^{182}W_{corrected} = \varepsilon^{182}W_{measured} - (1.41 \pm 0.05) \times \varepsilon^{183}W$$

and

$$\varepsilon^{182}W_{corrected} = \varepsilon^{182}W_{measured} - (-0.12 \pm 0.06) \times \varepsilon^{184}W,$$

respectively. Note that these correlations are obtained without correcting the leachate data for potential $^{182}$Hf decay. We have omitted this decay correction for several reasons. First, the lack of unprocessed aliquots for this study did not allow the determination of Hf/W ratios in the leachates, which are a prerequisite for this correction. Second, compared to the size of the nucleosynthetic anomalies (up to $-60$ $\varepsilon^{182}$W) the decay contribution to $\varepsilon^{182}$W is expected to be small (mostly within the analytical uncertainties), such that the decay correction most likely would not significantly affect the slopes of the regressions. This claim is further supported by the good correlation coefficient ($R^2 = 0.99$ for $\varepsilon^{182}$W vs. $\varepsilon^{183}$W data) of the decay-uncorrected data and the narrow range of $\varepsilon^{182}$W values obtained when applying the anomaly corrections derived above to each leachate point (Table 1). Third, even if the Hf/W ratios of the leachates were known, they are likely hampered by the incongruent dissolution of Hf and W during leaching, which would lead to inaccurate decay corrections (Burkhardt et al., 2012b). Forth, it is not clear whether $^{182}$Hf is homogeneously distributed at the scale sampled by the leachates and thus a correction with a canonical $^{182}$Hf/$^{180}$Hf might lead to under- or over-corrections of the leachate data. To further test the possible effects of the neglected $^{182}$Hf decay correction on the slopes we performed a Monte–Carlo simulation. For this, the individual leachate data were corrected for $^{182}$Hf decay using randomly generated Hf/W ratios (from 0.25 to 3.22 times the chondritic value and the canonical $^{182}$Hf/$^{180}$Hf of $(1.018 \pm 0.043) \times 10^{-4}$ (Kruijer et al., 2014)). The results were then regressed using ISOPLOT. Out of 50 runs, the MSWD values of the 'decay-corrected' slopes are in all but two cases worse than the ones of the uncorrected data and all the initial $\varepsilon^{182}$W values are below the initial solar system value. This implies that the simulations significantly over-corrected the actual decay and introduced excess scatter into the data. Notwithstanding these effects, the simulated slopes ($1.40 \pm 0.08$ (2 s.d.) and $-0.05 \pm 0.18$, respectively) cover the same limited range as the slopes obtained from the uncorrected data, providing further evidence for the robustness of the uncorrected data. Finally, the models of *s*-process nucleosynthesis can be fitted simultaneously to both the $^{186}$W/$^{184}$W as well as the $^{186}$W/$^{183}$W normalized uncorrected leachate data by varying the *s*-process yield

of a single W isotope (*cf.* Section 4.2). This would not be expected, if the slopes of the best-fit lines were significantly influenced by $^{182}$Hf decay, because it would affect the two normalization schemes differently. In addition, new high-precision W CAI data that was iteratively corrected for decay and nucleosynthetic anomalies yield identical and equally precise correlations of $\varepsilon^{182}W_{corr} = \varepsilon^{182}W_{measured} - (1.41 \pm 0.06) \times \varepsilon^{183}W$ and $\varepsilon^{182}W_{corr} = \varepsilon^{182}W_{measured} - (-0.11 \pm 0.05) \times \varepsilon^{184}W$ (Kruijer et al., 2014), thereby providing independent confirmation for the validity of the anomaly correction relations obtained here. Applying our correction equations to the CAI data of Burkhardt et al. (2008) and Kruijer et al. (2014) returns a bulk CAI isochron defining a solar system initial $^{182}Hf/^{180}Hf = 1.018 \pm 0.044 \times 10^{-4}$ and an initial $\varepsilon^{182}W = -3.49 \pm 0.11$, identical to and equally precise as the best estimates obtained by Kruijer et al. ($1.018 \pm 0.043 \times 10^{-4}$ and $-3.49 \pm 0.07$) using iterative correction methods.

### 4.4. Carrier phases of anomalous W

For a given meteorite, the W *s*-process excess signature is most prominent in the leachate residues (step 5). The insoluble residues remaining after acid leaching are enriched in refractory presolar oxides, graphite, diamond and SiC. Therefore, one or more of these phases qualify as the carrier of *s*-process W, which is likely embedded in the host minerals as WC or W metal (Lodders and Fegley, 1995). Avila et al. (2012) demonstrated that SiC grains contain *s*-process W. This is qualitatively consistent with what is observed here. The *s*-process enrichment measured for step 5 decreases from Orgueil via Murchison to Allende, while the SiC abundance in these meteorites decreases in the same order (14 ppm, 9 ppm and 0.01 ppm; Huss et al., 2003; other authors report different SiC abundances, however the abundance ratios between the different meteorites remain about the same; *e.g.*, Davidson et al., 2014). Using mass balance consideration, the low SiC abundance in Allende should not result in measurable anomalies. Taking the conservative assumptions of a 50 × solar W concentration (more realistic is probably <10 × solar; Avila et al., 2012) and pure *s*-process W in SiC requires ~7 ppm SiC to generate a −1 $\varepsilon^{183}$W anomaly. This suggests the presences of other carriers than SiC that are also involved in generating W isotope anomalies in the leachates. The W isotope data of Orgueil and Allende indicate that excess *s*-process W is already released in step 2 ($HNO_3$) (Fig. 5). This is unlikely the result of SiC etching because in this case, one would also expect a *s*-process excess in Murchison leachate 2 and this is not observed. More likely, the *s*-process signature in step 2 of Orgueil and Allende is caused by an additional *s*-process carrier, for example a (presolar) sulfide.

The *r*-excess/*s*-deficit signatures exhibited by leachates of Orgueil and Murchison represent a complementary reservoir to the *s*-process carriers. These signatures may be due to an easily dissolvable *r*-process carrier phase or in analogy to Mo, more likely represent the lack of dissolution of *s*-process carriers in these leachates and thus rather point to a *s*-depleted "homogenized" nebular component (Dauphas et al., 2002a; Schönbächler et al., 2005).

In summary, the observed nucleosynthetic variations in leachates of Orgueil, Murchison and Allende can be explained by admixing of *s*-process W carriers to *s*-process depleted/*r*-process enriched nebular components. In the likely case that more than one *s*-process carrier is present, the different carriers seem to have – on average – formed in a similar stellar regime. This does not exclude that some gains (that do not significantly contribute to the average W compositions of the grain population) formed in very specific and variable stellar environments as testified by single presolar grain data.

### 4.5. Comparisons to Zr and Te isotope data obtained on the same leachates and to results of other leachate studies

Leachate data from primitive chondrites are available from various studies and for a large number of elements. Most of the studies applied slightly varying procedures (*e.g.*, different acids and acid molarities, leaching times and temperatures) and for this reason, a direct quantitative comparison of the results is in most cases not warranted. Nevertheless, several key observations can be made. A common qualitative progressive trend from a *s*-deficit in the early leachate to a *s*-excess in the residues is observed for many elements (*e.g.*, Sr, Zr, Mo, Ru, Ba, Nd, Sm, Hf and W; *c.f.* Qin et al. (2011) and Burkhardt et al. (2012a)) in Murchison leachates. This most likely indicates the presence of common *s*-carriers for these elements in this meteorite. Notable exceptions from this trend are the highly siderophile elements Os (Reisberg et al., 2009) and Ru (Fischer-Gödde et al., 2014), whose more variable leachate patterns are either explained by different primary presolar carrier phases for those elements and/or their redistribution from a common carrier in the solar nebula or on the parent body (Yokoyama et al., 2011). Further it is observed that the anomaly release patterns (and not only the magnitude of the anomalies) can significantly vary for leachates from distinct meteorite types and that these differences may not be correlated. The information to be taken out of this complexity is that the processes acting on the carriers in the nebula and on the parent body result in different signatures for different elements. For disentangling these processes it is best to concentrate on data obtained from one set of leachate experiments. The leachates processed here for W isotopes were previously analyzed for their Zr (Schönbächler et al., 2005) and Te (Fehr et al., 2006) isotope compositions, which enables a direct quantitative comparison for at least these elements. For Te no significant nucleosynthetic anomalies were resolved (besides a potential small anomaly for Murchison leach step 2). This finding was interpreted to reflect efficient mixing of the moderately volatile Te in the gas phase of the solar nebula and a low Te concentration in remaining refractory presolar carrier phases. Given the different cosmochemical properties of Te and W, it is thus not surprising that the leachate data are not correlated for these elements. For the refractory lithophile element Zr, the leachates of the investigated meteorites show nucleosynthetic isotope variations, progressively changing from

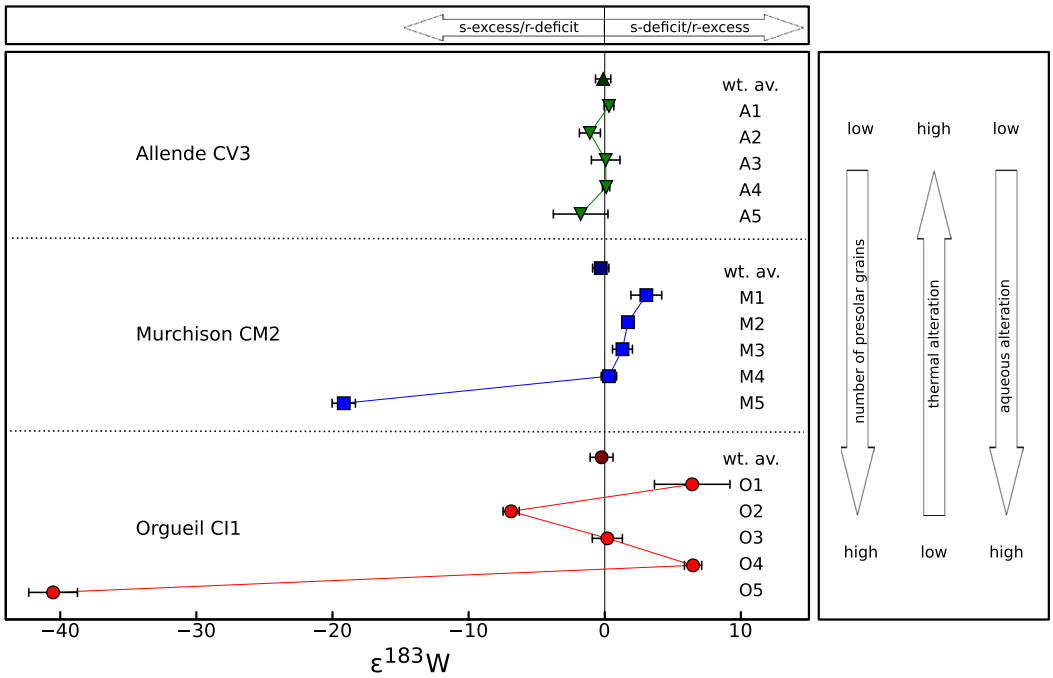


Fig. 5. $\varepsilon^{183}W$ values of Orgueil, Murchison and Allende leachates and their weighted averages. A general decrease of the size of the anomalies from CI1 > CM2 > CV3 indicates progressive destruction of presolar carriers with increasing thermal alteration on the parent bodies. However the different chondrites also exhibit variable anomaly patterns, indicating multiple carriers and potential nebular processing of presolar materials.

a *s*-deficit in the initial leachate to a *s*-excess in the final dissolution step. The *s*-process excesses in the last steps were mainly attributed to presolar SiC from AGB stars, which can contain significant amounts of Zr in ZrC subgrains (Amari et al., 1995) and exhibit strong enrichments in *s*-process Zr (Nicolussi et al., 1997). Following mass-balance arguments Schönbächler et al. (2005) inferred that besides SiC there must be at least one additional carrier of anomalous Zr, either a silicate (or other robust phase) with an *s*-excess signature or an easily leachable phase with a *s*-deficit/*r*-excess signature.

The Zr and W isotope anomalies of the leachates are related in the sense that the last leach step is dominated by a *s*-excess signature with increasing magnitude from CV3 to CM2 and CI chondrites, pointing toward SiC as a common *s*-process carrier for both elements. Furthermore, for Murchison all the leachates are correlated in the W and Zr isotope space (Fig. 6), indicating simple mixing relations between common *s*-process poor and *s*-process rich end-members with variable Zr/W ratios (in Fig. 6, mixing between average solar Zr and W and an end-member with higher than solar Zr/W results in a shallow slope while mixing with an end-member with sub-solar Zr/W results in a steep slope). Besides SiC and other refractory mineral phases with a high Zr/W, the mixture likely involves presolar silicates carrying a *s*-process excess signature and a complementary *s*-depleted easy leachable 'homogenized nebular component'. In contrast to the Murchison trend, the W and Zr isotope patterns for the Orgueil and Allende leachates are not correlated (Fig. 6), despite the similar elemental release ratios. This implies that the anomalous Zr and W now reside in separate carrier phases. The origin of the disparate Zr and W isotope signatures in the different meteorites could have been established by processing presolar Zr and W carriers in the solar nebula or on the meteorite parent body, or a combination of both.

### 4.6. Processing of presolar materials – nebular vs. parent body?

The mineralogical, petrological and chemical composition of chondritic meteorites and their components bear witness of complex physico-chemical processing and fractionation of materials in the solar nebula and on the meteorite parent bodies. The processing, distribution and fate of presolar materials in these settings, however, are still not well understood. While there is general agreement that variations in presolar grain abundances within a given meteorite class reflect different degrees of parent body metamorphism, it is debated whether different chondrite classes initially sampled identical or different blends of presolar materials, *i.e.*, whether significant nebular processing of presolar materials took place (*e.g.*, Huss, 2004; Yokoyama et al., 2011; Davidson et al., 2014). Such nebular processing was proposed to explain the presence of bulk scale nucleosynthetic isotope anomalies in some elements (*e.g.*, Trinquier et al., 2009). This, however, was questioned by others because of the lack of related bulk-scale anomalies in other elements (*e.g.*, Yokoyama et al., 2007, 2011). By comparing bulk meteorite and leachate data of Mo

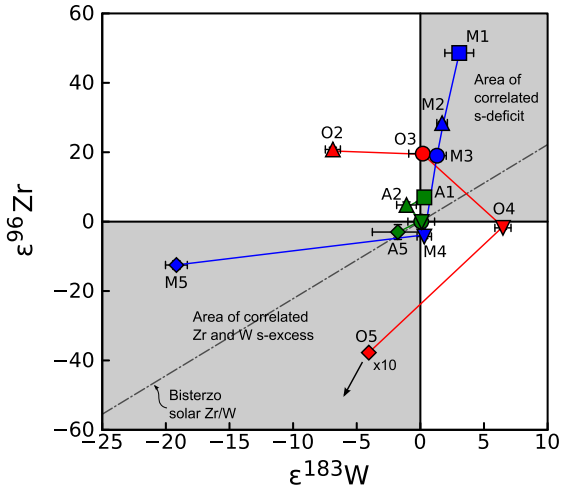


Fig. 6. $\varepsilon^{96}$Zr vs. $\varepsilon^{183}$W diagram for Orgueil, Murchison and Allende leachates. Symbols are as in Fig. 2. The dash-dotted line represents the mixing line between terrestrial W and Zr and a presumed *s*-process component, calculated using the *s*-process compositions of Bisterzo et al. (2011) and a solar Zr/W ratio. Gray area represents zones of correlated Zr and W *s*-process excess and deficit, respectively. Besides leach step 5, which exhibits *s*-process excesses for all meteorites, only the Murchison leachates show correlated Zr and W isotope variations, with leach M1-3 and M5 suggesting dissolution of common Zr and W anomaly carriers with sub-solar and super-solar Zr/W, respectively. The non-correlated leachates of Orgueil and Allende imply separate carriers of anomalous Zr and W in these meteorites. Anomalies of Orgueil leachate 5 were divided by 10 to fit scale. Zirconium isotope data from Schönbächler et al. (2005). Orgueil leach 1 is not shown because no Zr datum was obtained for this sample.

and W, Burkhardt et al. (2012a) suggested a thermal processing and mixing model of presolar materials in the nebula that can explain both, the presence of nucleosynthetic bulk anomalies for some elements, and their absence for others.

The new leachate data show evidence for nebular and parent body processing of presolar W (and Zr) that is consistent with a nebular thermal processing scenario for the origin of bulk scale nucleosynthetic anomalies. The abundances of presolar grains in the analyzed chondrites decreases with increasing thermal alteration and decreasing matrix abundance: CI1 > CM2 > CV3 (Huss, 2004). The general magnitude of the anomalies also decreases in this order (Fig. 5). This observation is qualitatively consistent with the notion of the progressive destruction of an initially homogeneous mixture of presolar grains by parent body processing. The correlation between parent body alteration and anomaly sizes also holds if the different matrix abundances of the chondrites and slight variations in the W release (Fig. 1) are taken into account. Thus the leachate data provide strong evidence for progressive destruction of presolar W (and Zr) carriers during parent body thermal metamorphism. However, both the relative magnitude of the leachate anomalies and the detailed anomaly release patterns vary for the three chondrites (Fig. 5). This is particular evident for leach step 2, which shows a W *s*-process excess for Orgueil and Allende, but a deficit for Murchison. This may either be the result of alteration on the parent body, *i.e.,* the redistribution of anomalous W into a new phase, and/or the fingerprint of dust processing in the nebula, which would imply that not all chondrites accreted the same blend of presolar materials.

The leachate data provide evidence for W redistribution on the parent body. Although the overall *elemental* W release patterns are similar for the three chondrites (Fig. 1), the complementary release pattern of step 1 and 5 suggest that some W was redistributed from refractory materials (step 5) to easy leachable phases (step 1) with increasing thermal parent body alteration. For example, by altering *s*-process enriched refractory metals, silicates, oxides or SiC in the parent body through aqueous fluids at elevated temperatures, anomalous W can move into easy leachable compounds like tungstenite, ferritungstite or scheelite. Such a process could also explain the *s*-excess excursion observed for leachate 2 of Orgueil and Allende. However, given that thermal and aqueous alteration of Murchison is intermediate to that Orgueil and Allende, it is unclear why Murchison does not exhibit this *s*-excess excursion in step 2. Taken at face values, this requires more severe W redistribution in Orgueil and Allende than in Murchison (or vice versa) during parent body processing. This seems unlikely considering the degrees of thermal and aqueous alteration of the meteorites. Instead this observation suggests that nebular processes also may have been important.

Within a nebular processing scenario, the following speculative and non-unique scenario can explain the observations: An initially homogeneous mix of various presolar materials is processed in different nebular settings (*e.g.*, changing oxygen fugacity), thereby locally redistributing isotopically anomalous W into new phases (*e.g.*, sulfides). The nebular redistribution of W did not inflict significant loss of anomalous W from the system, such that the overall W isotope composition remains virtually constant in most nebular regions. Hence, the redistribution must have occurred on a small scale. The chondrites, which accreted from this variably processed material, thus collected various carriers of anomalous W, but display no bulk isotope heterogeneities. Additional W redistribution by parent-body alteration processes, resulted in the final anomaly patterns observed for the leachates. It is noteworthy that the only known bulk planetary samples with resolvable nucleosynthetic W isotope variations (*s*-process deficits) are the volatile depleted IVB iron meteorites. This suggests that the *s*-process W depletion in these meteorites is related to the extreme volatile depletion, consistent with the lack of, *e.g.*, an anomalous sulfide phase in the materials that accreted to form the IVB iron parent body.

Nebular processes can affect W differently compared to other elements, *e.g.*, because some elements might be more volatile, and therefore were easier lost to the gas phase, or because they were strongly enriched in a specific carrier, which was preferentially fractionated in the nebula. The magnitude of the primordial nucleosynthetic anomaly as well as the concentration of a specific element in a carrier phase are also important parameters, which influence the

size and detectability of nucleosynthetic variations of an element. To explain the various correlated and uncorrelated isotope variations in leachates and the presence or absence of correlated or uncorrelated bulk scale nucleosynthetic anomalies requires both, the parent-body and nebular processing of planetary materials.

## 5. CONCLUSIONS

The W isotope data obtained here for the sequential digestion of the carbonaceous chondrites Orgueil (CI1), Murchison (CM2) and Allende (CV3) contain information about W nucleosynthesis, the correction of nucleosynthetic anomalies for Hf–W dating, the carrier inventory of the solar nebula and the processing of presolar material in nebular and parent-body settings.

The high precision *s*-excess/*s*-deficit mixing relationships obtained from the leachates provide a validity test for *s*-process nucleosynthesis models aiming to reproduce the solar *s*-process pattern in the Hf–Ta–W–Os mass region. Current *s*-process models provide qualitatively reasonable results, but in detail they differ from each other and the leachate data.

The correlations defined by the leachate data also provide a precise mean to correct nucleosynthetic anomalies that influence the Hf–W dating system. The correction relationships obtained here for the leachates are identical to the ones obtained based on CAI (Kruijer et al., 2014) and independently validate the CAI based revised initial solar system $^{182}Hf/^{180}Hf$ of $1.018 \pm 0.043 \times 10^{-4}$ and $\varepsilon^{182}W$ of $-3.49 \pm 0.07$.

Several carrier phases of anomalous W must be present in the chondrites to explain the leachate data. Alongside SiC grains as a common carrier for *s*-process W and Zr, and a homogenized nebular component with a *s*-deficit signature, our data indicate a $HNO_3$ leachable W phase with an *s*-excess signature, *e.g.*, a sulfide, and possibly silicates with Zr and W *s*-excess signature.

While the overall amplitude of the anomalies decreases with increasing thermal alteration experienced on the parent body (CI1 > CM2 > CV3.2), the differences in the leachate anomaly patterns between the meteorites suggest that nebular processes may also have played a role in addition to parent-body alteration. These processes affected the specific carriers and elements differently, resulting in the diverse nucleosynthetic signatures observed in meteoritic matter today. There is compelling evidence that variable nebular processing is responsible for the bulk scale nucleosynthetic anomalies observed in some elements; and their absence in others.

## ACKNOWLEDGMENTS

We thank L. Qin, an anonymous reviewer and the associate editor M. Boyet for constructive comments and the editorial handling of the manuscript. M. Lugaro freely shared unpublished *s*-process W yields and patiently answered our questions on *s*-process modelling. T. Kleine generously provided MC-ICPMS time at the WWU Münster, where T. Kruijer, M. Fischer-Gödde and D. Cook helped with setting up the MS for the measurement session.

## REFERENCES

Akram W., Schönbächler M., Sprung P. and Vogel N. (2013) Zirconium-hafnium isotope evidence from meteorites for the decoupled synthesis of light and heavy neutron-rich nuclei. *Astrophys. J.* **777**(169), 12pp.

Akram W., Schönbächler M., Bisterzo S. and Gallino R. (2015) Zirconium isotope evidence for the heterogeneous distribution of s-process materials in the solar system. *Geochim. Cosmochim. Acta*. http://dx.doi.org/10.1016/j.gca.2015.02.013.

Amari S., Lewis R. S. and Anders E. (1994) Interstellar grains in meteorites: I. Isolation of SiC, graphite and diamond; size distribution of SiC and graphite. *Geochim. Cosmochim. Acta* **58**, 459–470.

Amari S., Hoppe P., Zinner E. and Lewis R. S. (1995) Trace-element concentrations in single circumstellar silicon carbide grains from the Murchison meteorite. *Meteoritics* **30**, 679–693.

Amelin Y., Kaltenbach A., Iizuka T., Stirling C. H., Ireland T. R., Petaev M. and Jacobsen S. B. (2010) U–Pb chronology of the Solar System's oldest solids with variable $^{238}U/^{235}U$. *Earth Planet. Sci. Lett.* **300**, 343–350.

Andreasen R. and Sharma M. (2007) Mixing and homogenization in the early solar system: clues from Sr, Ba, Nd, and Sm isotopes in meteorites. *Astrophys. J.* **665**, 874–883.

Avila J. N., Lugaro M., Ireland T. R., Gyngard F., Zinner E., Cristallo S., Holden P., Buntain J., Amari S. and Karakas A. (2012) Tungsten isotopic compositions in Stardust SiC grains from the Murchison meteorite: constraints on the s-process in the Hf–Ta–W–Re–Os region. *Astrophys. J.* **744**, 49.

Bisterzo S., Gallino R., Staniero O., Cristallo S. and Käppeler F. (2011) The s-process in low-metallicity stars – II. Interpretation of high-resolution spectroscopic observations with asymptotic giant branch models. *Mon. Not. R. Astron. Soc.* **418**, 284–319.

Bisterzo S., Travaglio C., Gallino R., Wiescher M. and Käppeler F. (2014) Galactic chemical evolution and solar s-process abundances: dependence on the $^{13}C$-pocket structure. *Astrophys. J.* **787**. http://dx.doi.org/10.1088/0004-637X/787/1/10.

Bisterzo S., Gallino R., Käppeler F., Wiescher M., Imbriani G., Staniero O., Cristallo S., Görres J. and deBoer R. J. (2015) The branchings of the main s-process: their sensitivity to α-induced reactions on $^{13}C$ and $^{22}Ne$ and to the uncertainties of the nuclear network. *Mon. Not. R. Astron. Soc.* **449**, 506–527.

Boyet M. and Gannoun A. (2013) Nucleosynthetic Nd isotope anomalies in primitive enstatite chondrites. *Geochim. Cosmochim. Acta* **121**, 652–666.

Burkhardt C., Kleine T., Bourdon B., Palme H., Zipfel J., Friedrich J. M. and Ebel D. S. (2008) Hf–W mineral isochron for Ca, Al-rich inclusions: age of the solar system and the timing of core formation in planetesimals. *Geochim. Cosmochim. Acta* **72**, 6177–6197.

Burkhardt C., Kleine T., Oberli F., Pack A., Bourdon B. and Wieler R. (2011) Molybdenum isotope anomalies in meteorites: constraints on solar nebula evolution and origin of the Earth. *Earth Planet. Sci. Lett.* **312**, 390–400.

Burkhardt C., Kleine T., Dauphas N. and Wieler R. (2012a) Origin of isotopic heterogeneity in the solar nebula by thermal processing and mixing of nebular dust. *Earth Planet. Sci. Lett.* **357–358**, 298–307.

Burkhardt C., Kleine T., Dauphas N. and Wieler R. (2012b) Nucleosynthetic tungsten isotope anomalies in acid leachates of the Murchison chondrite: implications for Hf–W chronometry. *Astrophysical J. Lett.* **753**, L6.

Chen J. H., Papanastassiou D. A. and Wasserburg G. J. (2010) Ruthenium endemic isotope effects in chondrites and differentiated meteorites. *Geochim. Cosmochim. Acta* **74**, 3851–3862.

Chen H., Lee T., Lee D., Shen J. J. and Chen J. (2011) $^{48}$Ca heterogeneity in differentiated meteorites. *Astrophysical J. Lett.* **743**, L23.

Clayton D. D. (1982) Cosmic chemical memory – a new astronomy. *Q. J. Roy. Astron. Soc.* **23**, 174.

Dauphas N., Marty B. and Reisberg L. (2002a) Molybdenum nucleosynthetic dichotomy revealed in primitive meteorites. *Astrophys. J.* **569**, 139–142.

Dauphas N., Marty B. and Reisberg L. (2002b) Molybdenum evidence for inherited planetary scale isotope heterogeneity of the protosolar nebula. *Astrophys. J.* **565**, 640–644.

Dauphas N., Remusat L., Chen J. H., Roskosz M., Papanastassiou D. A., Stodolna J., Guan Y., Ma C. and Eiler J. M. (2010) Neutron-rich chromium isotope anomalies in supernova nanoparticles. *Astrophys. J.* **720**, 1577–1591.

Davidson J., Busemann H., Nittler L. R., Alexander C. M. O. D., Orthous-Daunay F. R., Franchi I. A. and Hoppe P. (2014) Abundances of presolar silicon carbide grains in primitive meteorites determined by NanoSIMS. *Geochim. Cosmochim. Acta* **139**, 248–266.

Fehr M. A., Rehkämper M., Halliday A. N., Schönbächler M., Hattendorf B. and Günther D. (2006) Search for nucleosynthetic and radiogenic tellurium isotope anomalies in carbonaceous chondrites. *Geochim. Cosmochim. Acta* **70**, 3436–3448.

Fischer-Gödde M., Kleine T., Burkhardt C. and Dauphas N. (2014) Origin of nucleosynthetic isotope anomalies in bulk meteorites: evidence from coupled Ru and Mo isotopes in acid leachates of chondrites. *45th Lunar Planet. Sci. Conf.* Houston. #2409.

Gannoun A., Boyet M., Rizo H. and El Goresy A. (2011) $^{146}$Sm–$^{142}$Nd systematics measured in enstatite chondrites reveals a heterogeneous distribution of $^{142}$Nd in the solar nebula. *Proc. Natl. Acad. Sci.* **108**, 7693–7697.

Hidaka H., Ohta Y. and Yoneda S. (2003) Nucleosynthetic components of the early solar system inferred from Ba isotopic compositions in carbonaceous chondrites. *Earth Planet. Sci. Lett.* **214**, 455–466.

Huss G. R. (2004) Implications of isotopic anomalies and presolar grains for the formation of the solar system. *Antarct. Meteor. Res.* **17**, 132.

Huss G. R. and Lewis R. S. (1995) Presolar diamond, SiC, and graphite in primitive chondrites: abundances as a function of meteorite class and petrologic type. *Geochim. Cosmochim. Acta* **59**, 115–160.

Huss G. R., Meshik A. P., Smith J. B. and Hohenberg C. M. (2003) Presolar diamond, silicon carbide, and graphite in carbonaceous chondrites: implications for thermal processing in the solar nebula. *Geochim. Cosmochim. Acta* **67**, 4823–4848.

Kleine T., Mezger K., Munker C., Palme H. and Bischoff A. (2004) $^{182}$Hf–$^{182}$W isotope systematics of chondrites, eucrites, and martian meteorites: chronology of core formation and early mantle differentiation in Vesta and Mars. *Geochim. Cosmochim. Acta* **68**, 2935–2946.

Kleine T., Touboul M., Bourdon B., Nimmo F., Mezger K., Palme H., Jacobsen S. B., Yin Q. and Halliday A. N. (2009) Hf–W chronology of the accretion and early evolution of asteroids and terrestrial planets. *Geochim. Cosmochim. Acta* **73**, 5150–5188.

Krot A. N., Amelin Y., Bland P., Ciesla F. J., Connelly J., Davis A. M., Huss G. R., Hutcheon I. D., Makide K., Nagashima K., Nyquist L. E., Russell S. S., Scott E. R. D., Thrane K., Yurimoto H. and Yin Q. (2009) Origin and chronology of chondritic components: a review. *Geochim. Cosmochim. Acta* **73**, 4963–4997.

Kruijer T. S., Kleine T., Fischer-Gödde M., Burkhardt C. and Wieler R. (2014) Nucleosynthetic W isotope anomalies and the Hf–W chronometry of Ca–Al-rich inclusions. *Earth Planet. Sci. Lett.* **403**, 317–327.

Lee T., Papanastassiou D. A. and Wasserburg G. J. (1977) Aluminum-26 in the early solar system – fossil or fuel. *Astrophys. J.* **211**, L107–L110.

Lewis R. S., Ming T., Wacker J. F., Anders E. and Steel E. (1987) Interstellar diamonds in meteorites. *Nature* **326**, 160–162.

Lodders K. and Fegley B. (1995) The origin of circumstellar silicon carbide grains found in meteorites. *Meteoritics* **30**, 661–678.

Lugaro M., Davis A. M., Gallino R., Pellin M. J., Straniero O. and Käppeler F. (2003) Isotopic compositions of strontium, zirconium, molybdenum, and barium in single presolar SiC grains and asymptotic giant branch stars. *Astrophys. J.* **593**, 486–508.

Lugaro M., Heger A., Osrin D., Goriely S., Zuber K., Karakas A. I., Gibson B. K., Doherty C. L., Lattanzio J. C. and Ott U. (2014) Stellar origin of the $^{182}$Hf cosmochronometer and the presolar history of solar system matter. *Science* **345**, 650–653.

Moynier F., Day J. M. D., Wataru O., Yokoyama T., Bouvier A., Walker R. J. and Podosek F. A. (2012) Planetary-scale strontium isotopic heterogeneity and the age of volatile depletion of early solar system materials. *Astrophys. J.* **758**(45), 7pp.

Nicolussi G. K., Davis A. M., Pellin M. J., Lewis R. S., Clayton R. N. and Amari S. (1997) S-process Zirconium in presolar silicon carbide grains. *Science* **277**, 1281–1283.

Nicolussi G. K., Pellin M. J., Lewis R. S., Davis A. M., Amari S. and Clayton R. N. (1998) Molybdenum isotopic composition of individual presolar silicon carbide grains from the Murchison meteorite. *Geochim. Cosmochim. Acta* **62**, 1093–1104.

Nyquist L. E., Kleine T., Shih C. Y. and Reese Y. D. (2009) The distribution of short-lived radioisotopes in the early solar system and the chronology of asteroid accretion, differentiation, and secondary mineralization. *Geochim. Cosmochim. Acta* **73**, 5115–5136.

Ott U. and Begemann F. (1990) Discovery of s-process barium in the Murchison meteorite. *Astrophys. J.* **353**, L57–L60.

Podosek F. A., Prombo C. A., Amari S. and Lewis R. S. (2004) S-process Sr isotopic composition in presolar SiC from the Murchison meteorite. *Astrophys. J.* **605**, 960–965.

Qin L., Dauphas N., Wadhwa M., Markowski A., Gallino R., Janney P. E. and Bouman C. (2008) Tungsten nuclear anomalies in planetesimal cores. *Astrophys. J.* **674**, 1234–1241.

Qin L., Carlson R. W. and Alexander C. M. O. (2011) Correlated nucleosynthetic isotopic variability in Cr, Sr, Ba, Sm, Nd and Hf in Murchison and QUE 97008. *Geochim. Cosmochim. Acta* **75**, 7806–7828.

Regelous M., Elliott T. and Coath C. D. (2008) Nickel isotope heterogeneity in the early Solar System. *Earth Planet. Sci. Lett.* **272**, 330–338.

Reisberg L., Dauphas N., Luguet A., Pearson D. G., Gallino R. and Zimmermann C. (2009) Nucleosynthetic osmium isotope anomalies in acid leachates of the Murchison meteorite. *Earth Planet. Sci. Lett.* **277**, 334–344.

Rotaru M., Birck J. L. and Allègre C. J. (1992) Clues to early solar system history from chromium isotopes in carbonaceous chondrites. *Nature* **358**, 465–470.

Schönbächler M., Lee D. C., Rehkämper M., Halliday A. N., Fehr M. A., Hattendorf B. and Günther D. (2003) Zirconium isotope evidence for incomplete admixing of r-process components in the solar nebula. *Earth Planet. Sci. Lett.* **216**, 467–481.

Schönbächler M., Rehkämper M., Lee D.-C. and Halliday A. N. (2004) Ion exchange chromatography and high-precision isotopic measurements of zirconium by MC-ICPMS. *Analyst* **129**, 32–37.

Schönbächler M., Rehkämper M., Fehr M. A., Halliday A. N., Hattendorf and Günther D. () Nucleosynthetic zirconium

isotope anomalies in acid leachates of carbonaceous chondrites. *Geochim. Cosmochim. Acta* **69**, 5113–5122.

Trinquier A., Birck J. L. and Allègre C. J. (2007) Widespread $^{54}$Cr heterogeneity in the inner solar system. *Astrophys. J.* **655**, 1179–1185.

Trinquier A., Elliott T., Ulfbeck D., Coath C., Krot A. N. and Bizzarro M. (2009) Origin of nucleosynthetic isotope heterogeneity in the solar protoplanetary disk. *Science* **324**, 374–376.

Vockenhuber C., Oberli F., Bichler M., Ahmad I., Quitté G., Meier M., Halliday A. N., Lee D. C., Kutschera W., Steier P., Gehrke R. J. and Helmer R. G. (2004) New half-life measurement of $^{182}$Hf: improved chronometer for the early solar system. *Phys. Rev. Lett.* **93**(172501).

Völkening J., Köppe M. and Heumann K. (1991) Tungsten isotope ratio determination by negative thermal ionization mass spectrometry. *Int. J. Mass Spectr. Ion Proc.* **107**, 361–368.

Yokoyama T., Rai V. K., Alexander C. M. O., Lewis R. S., Carlson R. W., Shirey S. B., Thiemens M. H. and Walker R. J. (2007) Osmium isotope evidence for uniform distribution of s- and r-process components in the early solar system. *Earth Planet. Sci. Lett.* **259**, 567–580.

Yokoyama T., Alexander C. M. O. and Walker R. J. (2010) Osmium isotope anomalies in chondrites: results for acid residues and related leachates. *Earth Planet. Sci. Lett.* **291**, 48–59.

Yokoyama T., Alexander C. M. O. and Walker R. J. (2011) Assessment of nebular versus parent body processes on presolar components present in chondrites: evidence from osmium isotopes. *Earth Planet. Sci. Lett.* **305**, 115–123.

Zinner E. (2014) Presolar Grains. In *Treatise on Geochemistry (Second Edition)* (eds. Heinrich D. Holland and Karl K. Turekian). Elsevier, Oxford, pp. 181–213.

*Associate editor:* Maud Boyet